Integrated Proteomics and Metabolomics to Study IgA Nephropathy on Early Stage and Identification of Biomarkers

Di Zhang
Zhejiang Provincial People's Hospital, Hangzhou Medical College
Yaohan Li
Zhejiang University
Mingzhu Liang
Zhejiang Provincial People's Hospital, Hangzhou Medical College
Yan Liang
Zhejiang Provincial People's Hospital, Hangzhou Medical College
Jingkui Tian
The Cancer Hospital of the University of Chinese Academy of Sciences (Zhejiang Cancer Hospital), Chinese Academy of Sciences
Qiang He
the First Affiliated Hospital of Zhejiang Chinese Medical University (Zhejiang Provincial Hospital of Traditional Chinese Medicine)
Juan Jin (jinjuan@hmc.edu.cn)
Zhejiang Provincial People's Hospital, Hangzhou Medical College
Wei Zhu
The Cancer Hospital of the University of Chinese Academy of Sciences (Zhejiang Cancer Hospital), Chinese Academy of Sciences

Research Article

Keywords: IgA nephropathy, proteomics, metabolomics, biomarker, LASSO, plasma

Posted Date: October 20th, 2022

DOI: https://doi.org/10.21203/rs.3.rs-2177109/v1

Additional Declarations: No competing interests reported.

Version of Record: A version of this preprint was published at Clinical Proteomics on December 27th, 2022. See the published version at https://doi.org/10.1186/s12014-022-09387-5.

Abstract

Background

IgA nephropathy (IgAN) is the most common primary chronic glomerulopathy globally. For IgAN diagnosis, kidney biopsy is still the standard method, which is invasive. And there are no effective plasma biomarkers for the disease at the early stage. The research aimed to find potential biomarkers for diagnosing IgAN.

Methods

Plasma samples of 33 early-stage IgAN patients who were not taking hormonal drugs and 20 healthy controls were collected for proteomic and metabolomic analysis. The least absolute shrinkage and selection operator (LASSO) was used to construct a binary logistic regression model by combining proteomic and metabolomic data. The area under the curve (AUC) of the receiver operating characteristic (ROC) curve, sensitivity, and specificity test were performed to assess the model's performance.

Results

Proteomic analysis of IgAN plasma revealed that the complement and the immune system were activated. And the metabolomic result showed that energy and amino acid metabolism were disordered in IgAN patients. Through machine learning, PRKAR2A, IL6ST, SOS1, and palmitoleic acid have been identified as potential biomarkers. Based on the AUC value for the training and test sets, the classification performance was 0.994 and 0.977, respectively. The AUC of the external validation of the four biomarkers was 0.91.

Conclusion

In this study, we applied proteomics and metabolomics techniques to analyze the plasma of IgAN patients and find biomarkers. PRKAR2A, IL6ST, SOS1, and palmitoleic acid were combined to serve as potential biomarkers for early diagnosis of IgAN.

Introduction

IgAN, an autoimmune disease, is the most common primary glomerulonephritis worldwide and a significant cause of chronic kidney disease and kidney failure [1]. It has been reported that the incidence of IgAN varies from 0.2 to 5 per 100,000 individuals per year on different continents [2]. Glomerular mesangial cell proliferation and extracellular matrix expansion in IgAN patients begin at an early stage of disease and progress to glomerular and interstitial sclerosis, with approximately 30–40% of patients progressing to end-stage renal disease within 20 years [3]. Although the original description of IgAN has

been put forward for more than 50 years [4], the specific pathogenesis of IgAN is unclear. A global perspective of IgAN suggests that early therapy may reduce the global burden of end-stage kidney disease caused by IgAN[5]. Therefore, a simple and safe method for early diagnosis is in need.

Currently, the diagnosis and risk stratification of IgAN is based on kidney biopsy [6]. A combination of pathologic grading and clinical characteristics has been used to develop a model that can predict the prognosis of IgAN [7]. However, renal puncture biopsies are invasive, not reproducible, and may result in severe complications such as bleeding [8], which limits their use. Because of this, it is unsuitable for monitoring the progression of IgAN or screening to identify it in the early stage [9]. Therefore, a non-invasive diagnosis approach was needed for early diagnosis of IgAN even before the onset of reduced eGFR [10]. Some biomarkers for IgAN diagnosis have been reported in recent years. Abnormal glycosylated (galactose deficient) immunoglobulin A1 (GD-IGA1) induces an autoimmune response and deposition of immune complexes in the kidney as possible pathogenesis for IgAN, which can be a potential, noninvasive biomarkers of IgAN [11, 12]. A prospective cohort study has shown that the levels of serum platelet-derived growth factor DD (PDGF-DD) were explicitly elevated in patients with IgAN, particularly in those with early disease, which can serve as a biomarker of disease and/or disease activity [13]. However, Kidney Disease: Improving Global Outcomes (KDIGO) guidelines categorically state in a practice point that, to date, there are no validated blood or urine biomarkers for the diagnosis of IgAN [14]. Therefore, more research should be done to explore the pathogenesis of IgAN and potential biomarkers to distinguish it from healthy controls or other glomerular diseases.

In recent decades, omics-based technologies have provided new perspectives on nephropathy studies. The applications of omics, including genomics, transcriptomics, proteomics, and metabolomics, can help us understand basic physiological processes and identify biomarkers [15, 16]. Recently, mass spectrometry analysis of the urine proteome identified 14 different urinary protein fragments that belong to the region of the connecting peptide of the total fetuin-A protein, demonstrating the association of fetuin-A peptides with impaired kidney function in T2DM patients, and can be used as markers for kidney disease detection [17]. Using a peptidome database, David G. et al. defined 273 biomarkers and built an SVM classification model to distinguish healthy subjects from individuals with biopsy-proven kidney disease in the training set [18]. In another study, NMR-based metabolomics was applied for the urinary metabolic profile and could provide a differential diagnosis of primary focal segmental glomerulosclerosis (FSGS) and other glomerulopathies [19]. In IgAN, metabolomic profiling has found that glycine levels increased without reduced eGFR compared to healthy, membranous nephropathy (MN), minimal change disease (MCD), or lupus nephritis (LN) [20]. However, integrative multi-omics analysis was less applied in IgAN. Thus, we performed a multi-omics study on IgAN, which had the potential to provide insights into various aspects.

This study used a multi-omics workflow combining proteomics and metabolomics to identify the potential biomarkers for IgAN diagnosis. The plasma proteomics and metabolic characteristics of IgAN in the early stage were described. After filtering the variables with LASSO regression, logistic regression was applied to build the model based on the minor absolute shrinkage. Subsequently, four potential

biomarkers of IgAN were identified and evaluated using ROC curves. Finally, independent samples were used to validate biomarkers. These analyses will inform strategies for the early diagnosis of IgAN.

Methods And Materials

Study population

Samples of IgAN plasma were obtained from Zhejiang Provincial People's Hospital at the time of diagnostic renal biopsies performed. Patients with a pathologically confirmed IgAN diagnosis and not treated with hormone immunosuppressants were included. People without kidney dysfunction constructed the healthy control group. Fifty-three individuals (33 patients with IgAN and 20 healthy controls) were enrolled for proteomic and metabolomic analyses. And 19 people (9 patients with IgAN and 10 healthy controls) were tested by ELISA in the validation set. The ethics committee approved this study for clinical studies at Zhejiang Provincial People's Hospital. For plasma sampling, whole blood was collected in an EDTA tube and centrifugated at 1,000 g for 10 minutes. Plasma was collected after centrifugation and kept at -80℃ until processed.

Sample Preparation For Mass Spectrometry (Ms) Proteomic Analysis

Samples of plasma were processed according to the previously described procedure with modifications [22]. Briefly, 100 μg of the protein was purified by methanol/chloroform precipitation. After centrifugation, the supernatant was removed, and the protein precipitate was dried. Afterward, the sample was resuspended in 50 mM NH_4HCO_3 solution and reduced with dithiothreitol (0.25 M in 50 mM NH_4HCO_3) for 30 min at 56°C, then alkylated with 0.3 M chloroacetamide for 30 min at 37℃ in darkness. After alkylation, protein samples were diluted by adding 40 μL 100 mM NH_4HCO_3 and digested by trypsin at 37℃ for 16 hours (enzyme to protein ratio of 1:100). The digestion was terminated by adding 20 μL 0.1% formic acid. After that, the samples were then purified using Ziptip (Merck Millipore, MA) C18 cartridges according to standard procedures. Mixed peptides for quality control were prepared by mixing equal volumes of each sample.

Liquid Chromatography-tandem Mass Spectrometry (Lc-ms/ms) Analysis

An Orbitrap 480 (Thermo Fisher Scientific, Dreieich, Germany) coupled with an EASY-nLC 1200 (Thermo Fisher Scientific, Dreieich, Germany) was used to obtain mass spectral data. A binary mobile phase system was used, consisting of solvent A containing 0.1% formic acid in water and solvent B containing 80% acetonitrile in 0.1% formic acid/water. Elution for 65 min was performed by the following gradient: 0–1 minutes, 3%-5% B; 1–52 minutes, 8% – 40% B; 52–56 minutes, 40%-95% B; 56–65 minutes, 95% B. Data-independent acquisition (DIA) mode was used to detect the peptide ions.

Protein Identification From The Ms Data

For the construction of the spectral library, the mixed peptides were fractionated and analyzed by LC-MS/MS in DDA mode. The RAW data were processed on the Protein Discoverer (Thermo Fisher Scientific, Dreieich, Germany) software with database UP000005640 downloaded from Uniprot. The result was imported into Skyline, and the spectral library was constructed. For protein quantification, chromatograms were extracted from RAW files acquired in DIA mode, and the target FASTA file was using database UP000005640. MSstats-Input file was exported and further processed using the R package MSstats for protein quantification and group comparison.

Functional Analysis Of Proteins

Gene set enrichment analysis (GSEA) was performed using the Kyoto Encyclopedia of Genes and Genomes (KEGG) subset of canonical pathways gene set in the Molecular Signatures Database (MSigDB). The KEGG database (http://www.genome.jp/kegg/) was used to map differentially expressed proteins (DEPs) pathway mapping. The clusterprofiler R package was used to annotate DEPs according to Gene Ontology (GO) database. A protein-protein interaction (PPI) network was constructed using the STRING database (http://string-db.org) and drawn in Cytoscape 3.9.0.

Sample Preparation For Ms Metabolomics Analysis

The plasma sample (50 μL) was mixed with ketoprofen (internal standard, IS1) purchased by Makclin (Shanghai, China), Sulfamerazine (internal standard, IS2) purchased by aladdin (Shanghai, China), 2-chloro-L-phenylalanine (internal standard, IS3) purchased by Makclin (Shanghai, China), and 150 μL of methanol (MS grade). The mixture was kept at − 20℃ for 30 minutes and centrifuged at 14,000 g at 4℃ for 20 minutes. The supernatant was further dried in a vacuum centrifugal concentrator. The quality control (QC) sample was prepared by mixing an equal aliquot from each plasma sample. All samples were redissolved by methanol in water (v:v = 2:1) before MS detection.

Untargeted Metabolomics Assay

ACQUITY Ultra Performance Liquid Chromatography (UPLC) (Thermo Fisher Scientific, Dreieich, Germany) with Waters ACQUITY UPLC T3 C18 Column (2.1 mm x 100 mm, 1.8 um) was used to perform the separation at a flow rate of 0.30 mL/min. The injection volume was 8 μL, and the auto-sampler temperature was 4°C. Solvent A (0.1% formic acid in water) and solvent B (0.1% formic acid in acetonitrile) were applied as mobile phases. Within 20 minutes, the analytes were separated in gradient condition: 0–1 min, 1% B; 1–15 min, 2% ~ 98% B; 15–18 min, 98% B; 18–20 min, 98% ~ 2% B. A polarity-switching mass spectrometer operated by Thermo Scientific Orbitrap 480 was used to detect metabolites with the spray voltage of 3.5 kV and − 2.5 kV in positive and negative modes respectively. The normalized

collision energy of 35 was used, and the capillary temperature was 300 degrees Celsius. Data-dependent acquisition (DDA) was performed using a C-trap dissociation scan (HCD).

Metabolomics Data Processing

The acquired data were processed with Compound Discoverer 3.1 software (Thermo Fisher Scientific, Dreieich, Germany), including retention time correction, peak identification, peak extraction, peak integration, and peak alignment. Data were annotated by online databases KEGG, HMDB, mzCloud, and Chemspider. MetaboAnalyst (https://www.metaboanalyst.ca) was used to perform the principal component analysis. KEGG pathway databases and HMDB (https://hmdb.ca) were used to identify the top metabolic pathways associated with IgAN.

Machine Learning Analysis

The LASSO regression analysis was performed in R using the glmnet package and binary logistic regression to construct the diagnosis model. To further assess the performance of the diagnosis model, a 10-fold cross-validation was conducted. The ROC curve was used to evaluate the model diagnostic performance. And the diagnosis model was further verified by a support vector machine (SVM) and random forest.

Validation Of Potential Markers By Elisa Assays

To further validate the reliability of the combination biomarkers, biomarkers including PRKAR2A, IL6ST, SOS1, and palmitoleic acid were selected for targeted analysis by ELISA assays. The independent batch of samples including 9 plasma samples from the IgAN group, and 10 plasma samples from healthy people were used for the assays. They were measured by human PRKAR2A ELISA kit (PRKAR2A_AE1652A-96T, Chuangshi, Tianjin, China), human Gp130/IL6ST ELISA Kit (EK0367, BOSTER, California, USA), human SOS1 ELISA (EH12498-96T, FineTest, Wuhan, China) kit and human palmitoleic acid ELISA kit (CB15581-Hu, COIBO, Shanghai, China), respectively.

Statistics Analysis

Statistical analyses were conducted with the program R 4.1.0. Two-way unpaired Student's t-tests were used to compare two groups. Differences were considered significant at a $p < 0.05$.

Result

Study population

The research methodology comprised a preliminary finding driven by an integrated analysis of plasma proteomics and metabolomics of IgAN patients to identify the biomarkers and construction of a diagnostic model externally validated by a validation cohort (Supplemental Figure S1). IgAN patients were diagnosed by biopsy, and those not treated with hormone immunosuppressants were selected. A total of 20 normal controls and 33 patients with IgAN were enrolled. A summary of the demographic and clinical characteristics of study participants was presented in Supplement TableS1. The age in the IgAN group was 38.24 ± 13.16 years old, and the age in the control group was 39.85 ± 14.56 years old. There was no significant difference in the distribution of age and gender in the two groups. In comparison, creatinine (CRE) and uric acid (UA) showed different levels in the two groups, which served as biochemical markers of renal damage.

Igan Proteomic Analysis And Identification Of Deps

A total of 5267 proteins were identified. The quantified proteins are listed in Supplement TableS2. Proteins with more than 50% missing values were discarded, and 5255 proteins remained. After normalizing the intensity values of each sample, the median of differences between samples can be normalized almost on the same line as found in the box plot (Figure S2). Among the quantifiable proteins, 71 proteins exhibited a significant difference in IgAN compared to healthy controls (adjust $p < 0.05$, Supplement TableS3). Among them, 40 proteins were up-regulated and 31 were down-regulated, as demonstrated in Fig. 1A. Among the DEPs there were several proteins have been reported in the prediction of nephropathies, such as Immunoglobulin heavy variable 1–18 (IGHV1-18) [23], Beta-2-microglobulin (B2M) [24], Leucine-rich alpha-2-glycoprotein (LRG [25], and Aquaporin-1(APQ1) [26]. A hierarchical clustering algorithm was applied based on the top 20 DEPs (Fig. 1B). The result showed that the expression of DEPs could separate most IgAN samples from healthy controls.

Functional Enrichment Analysis

GSEA predicted significantly altered signaling pathways in IgAN according to the normalized enrichment score (NES). Complement and coagulation cascades and MTOR signaling pathway were enriched in the IgAN subgroup (Fig. 2). Further, GO analysis was performed to identify the major functional categories of DEPs. Classification of the proteins of biological process terms showed that the increased proteins in IgAN patients were mainly associated with abnormal immune processes, including complement activation and regulation of humoral immune response. (Fig. 3A). The down-regulated proteins were primarily involved in platelet aggregation, renal system process, and regulation of homotypic cell-cell adhesion (Fig. 3B). Detailed information was provided in Supplement TableS4. Next, KEGG pathway enrichment was performed. Complement and coagulation cascades, various types of N-glycan biosynthesis, and Valine and leucine, and isoleucine degradation were enriched (Fig. 3C). Next, with the STRING tool and Cytoscape, we analyzed the interaction network between these DEPs to understand their biological function and possible relationship better (Fig. 3D). These data demonstrated that several

metabolic pathways were altered in IgAN patients, and the complement immune system is significantly activated among IgAN patients.

Differentially Abundant Metabolites Between Healthy Controls And Igan Patients

The metabolites with variable importance in projection (VIP) values greater than 1.0 and $p < 0.05$ were considered as differentially abundant metabolites (DAMs). 90 out of 540 metabolites were identified (Fig. 4C). 53 increased DAMs and 37 decreased DAMs were identified in the IgAN group (Fig. 4D). All the DAMs were annotated and classified into nine categories in the HMDB database. Information about the metabolites was listed in Supplement TableS5.

All annotation metabolites were then imported into MetaboAnalyst 5.0 for pathway analysis. The metabolome set enrichment analysis (MSEA) showed that glycolysis/gluconeogenesis, pyruvate metabolism, and amino acid metabolism were changed in IgAN. (Fig. 5A). And DAMs were mapped to the KEGG pathway to explore the metabolic alterations (Fig. 5B). The result showed that 17 metabolite pathways were changed, including carbohydrate, energy, and amino acid metabolism. A summary of the altered abundances of these pathways and metabolites was exhibited in Supplement TableS6. And a heatmap of the DAMs mapped on KEGG pathways was illustrated (Figure S4).

Construction Of The Diagnostic Model For Igan

Potential biomarkers of IgAN were then identified via comprehensive proteomic and metabolomic profiling. Exposomes and vitamin metabolites were excluded because vitamin supplements, medications, and dietary factors may affect metabolite levels independently of disease status. The DEPs and the rest of the DAMs were used for machine learning to build classification models. To verify the accuracy of the signature, the whole dataset was divided into the training set and the testing set in a ratio of 7:3. The LASSO regression model was used to determine the diagnostic markers of IgAN in the training set. Three unique proteins and one metabolite were identified as potential biomarkers, including PRKAR2A (P13861), IL6ST (P40189), SOS1(Q07889), and Palmitoleic acid. A ROC analysis was applied after calculating the predicted probabilities to evaluate the diagnostic accuracy of the four selected biomarkers. The AUC of the combination of these four biomarkers was 0.994 (Fig. 6A). In the test set, the four biomarkers also showed good diagnostic performance, and the AUC was 0.977 (Fig. 6B). Meanwhile, the four biomarkers can predict IgAN with high precision in the whole set, and the AUC was 0.992 (Fig. 6C). Next, we analyzed the levels of the biomarkers in all samples. There were significant changes in four biomarkers between IgAN and health control. The level of IL6ST was increased, while the levels of PRKAR2A, SOS1, and palmitoleic acid were decreased in the IgAN group. The levels of the four biomarkers were displayed in Figure S5. Based on ROC analysis, the four biomarkers yielded a diagnosis of IgAN, respectively, with a ROC > 0.8 (Fig. 6D). In short, these results showed that the combination of biomarkers significantly increased the predictive ability of the model. Additionally, random forest

classification and SVM were used to further validate the model retrieved from the cross-validation procedure. Supervised random forest classification using the four metabolites had a classification accuracy of 100%, and supervised SVM also showed a 100% accuracy (Table 1).

Table 1
Classification table of random forest method and SVM.

Random forest classification, accuracy = 100%, N = 51		
	Health	IgAN
Health	18	0
IgAN	0	33

Support vector machine classification, accuracy = 100%,N = 51		
	Health	IgAN
Health	18	0
IgAN	0	33

External Validation Of Biomarkers

An independent cohort of 10 healthy controls and 9 patients with IgAN was used for external validation of the four biomarkers. Demographic and clinical data of the study group was presented in Supplement TableS7. ELISA assays determined the content of the four biomarkers. The ROC curve showed that the diagnostic ability of the four biomarkers was 0.911 (Fig. 7). The result further proved that these three proteins and a metabolite were potential biomarkers for separating IgAN from health controls.

Discussion

IgAN was defined as a common type of primary glomerulonephritis [27]. And IgAN is one of the leading causes of end-stage renal disease [12]. The diagnosis was primarily based on changes in kidney pathology, and patients have heterogeneous characteristics and prognoses. Though aberrant glycosylation [28], circulating immune complex deposition [29], and immune cell infiltration [30] were reported to be involved in the IgAN, the pathogenesis of IgAN has not been fully elucidated. In this study, through proteomics and metabolomics, we found that various metabolic pathways were disturbed in the early stage of IgAN.

Proteins Associated With Complement In Igan Plasma

Blood protein analysis is an important clinical application of proteomics, but its dynamic range presents a challenge. Proteome in-depth analysis is necessary for identifying low-abundance proteins in experiments. So DIA mode was used to perform proteomic analysis on samples [31]. In this study, 71 DEPs were identified in the IgAN by DIA proteomic analysis. These proteins play a critical role in complement activation and humoral immune response. Complement activation has apparent alterations in IgAN patients. Excessive complement activation may be involved in crescent formation, predominantly diffuse crescent formation [32]. We found that complement-associated proteins have been activated in early-stage IgAN patients, even though the value of eGFR was normal.

Amino Acid Metabolism Of Dams In Igan Plasma

Between IgAN patients and healthy individuals, we detected a series of dysregulated amino acid metabolism. Among them, tryptophan, kynurenine, and ornithine were increased. Metabolic disturbances of amino acids were also observed in another IgAN metabolomics study, in which alanine, glycine, and isoleucine levers were significantly up-regulated [20]. Besides, tryptophan was an essential amino acid for an organism's energy metabolism and was a precursor material for 5-hydroxytryptamine and kynurenine [36]. The kynurenic acid pathway was thought to be the main catabolic route for tryptophan [37]. The metabolism of tryptophan was related to the production of urine toxin in chronic kidney disease and impaired renal function in diabetic nephropathy, which promotes oxidation, inflammation, coagulation, and apoptosis [38, 39]. Metabolomics results showed abnormal tryptophan metabolism in IgAN patients, with significantly elevated levels of 5-hydroxyindoleacetate and kynurenine. Therefore, amino acid metabolism dysregulation also existed in IgAN patients and influenced the process of the disease.

Biological Functions Of Biomarkers

Considering the clinical feasibility for early diagnosis of IgAN, a concise multi-omic classifier containing PRKAR2A, IL6ST, SOS1, and palmitoleic acid was created. PRKAR2A is the protein kinase cAMP-dependent type II regulatory subunit alpha and has been reported to play a core role in regulating neuroinflammatory processes [40]. Several studies suggested that PRKAR2A was associated with inflammatory pain and that antagonizing PRKAR2A offered a practical solution to controlling inflammatory pain [41, 42]. In this study, down-regulated plasma PRKAR2 was observed among IgAN patients. The changes indicated that the decrease of PRKAR2A plays a role in the early stage of IgAN, and it can be further studied as a biomarker for regular screening of IgAN patients. IL6ST, also name gp130, is the signaling subunit of receptors for cytokines of the IL-6 family [43] and plays a crucial role in maintaining immunity, mediating immune responses, and regulating inflammation [44]. In vivo, selective inhibition of trans signal transduction by a fusion protein containing two soluble forms of gp130(sgp130) chains linked by an inactivated Fc receptor portion (sgp130Fc) alleviated disease progression in rapidly progressive glomerulonephritis mice [45]. In vitro studies revealed that inhibition of

IL6ST expression could reduce the level of fibrosis-related genes in HG-treated cells [46]. According to our results, in IgAN patients, the level of IL6ST was significantly higher than that in healthy controls. Therefore, the results showed that IL6ST can distinguish IgAN from health and can be biomarkers for further study. SOS-1 is a guanine nucleotide exchange factor for RAS proteins. The expression of SOS1 can affect intracellular ROS levels, and the loss of SOS1 leads to specific changes in mitochondrial shape, mass, and dynamics, resulting in energy metabolism disorders [47]. A previous study showed that Ras-Sos-1 was suggested to play a significant role in regulating renal tubular epithelial-to-mesenchymal transition [48]. This study found that the expression of SOS-1 was significantly reduced in IgAN. Additionally, metabolomic data suggested dysregulation of energy metabolism in IgAN patients indicating SOS-1 may thus be a robust diagnostic biomarker for IgAN. Palmitoleic acid is an omega-7 monounsaturated fatty acid (MUFA) [49]. Incubation with palmitoleate can reverse the proinflammatory gene expression and cytokine secretion seen in bone marrow-derived macrophages from high fat-fed mice [50]. A clinical study found that patients with end-stage renal disease have lower palmitoleic acid levels than the control group [51]. This study found that the content of palmitoleic acid was also deficient in early-stage IgAN patients, suggesting it might be the potential biomarker of IgAN.

Limitations And Future Perspectives

This study is still subject to some limitations. First of all, we only included a few patients in this study. These findings require further validation using large sample sizes. Second, these results were obtained under laboratory conditions; the robustness, accuracy, and quantification must be further validated. Third, more research is required to explore the pathophysiologic mechanisms underlying these biomarkers for identifying therapeutic targets.

Conclusion

In summary, integrative DIA proteomics and untargeted metabolomics analyses of plasma were performed to construct the IgAN diagnosis biomarkers panels. Proteomic analysis of IgAN plasma revealed that the complement and the immune system were activated. And the metabolomic result showed that energy and amino acid metabolism were disordered in IgAN patients. Four potential biomarkers, PRKAR2A, IL6ST, SOS1, and palmitoleic acid, were selected by LASSO, which can be used as early warning and diagnosis of IgAN.

List Of Abbreviations

IgAN	IgA nephropathy
LASSO	Last absolute shrinkage and selection operator
AUC	Aea under the curve
ROC	Rceiver operating characteristic curve
DIA	Data-independent acquisition
FSGS	Focal segmental glomerulosclerosis
MN	Membranous nephropathy
MCD	Minimal change disease
LN	Lupus nephritis
LC-MS/MS	Liquid chromatography-tandem mass spectrometry
DEPs	Dferentially expressed proteins
DAMs	Differentially abundant metabolites

Declarations

Acknowledgements

The authors acknowledge the technicians who performed proteomic and metabolomic analyses of plasma samples and those responsible for providing plasma samples. The authors acknowledge using instruments at the Shared Instrumentation Core Facility at the Institute of Basic Medicine and Cancer (IBMC), Chinese Academy of Sciences.

Authors' contributions

JJ, WZ, YL, DZ contributed to the research idea and study design. YL, DZ contributed analysis tools and helped to provide methodology guidance. JJ, ZW, YL contributed to the methodology and reviewed the manuscript. YL, ZD contributed to the manuscript writing and revision. JT, QH, JJ, WZ contributed to the project administration, funding acquisition, and resources. DZ contributed to the data analysis by software. All authors contributed to editing the manuscript. All authors read and approved the final manuscript.

Found

This research was supported by the Huadong Medicine Joint Funds of the Zhejiang Provincial Natural Science Foundation of China(Grant No. LHDMZ22H050001); the Construction of Key Projects by Zhejiang Provincial Ministry(Project No.WKJ-ZJ-2017), The Zhejiang Province Chinese Medicine Modernization Program(Project No. 2020ZX001), The Key Project of Scientific Research Foundation of

Chinese Medicine (2022ZZ002) the "Pioneer" and "Leading Goose" R&D Program of Zhejiang(2022C03118); The Key project of Basic Scientific Research Operating Funds of Hangzhou Medical College(KYZD202002).

Availability of data and materials

All data generated or analyzed during this study are included in this published article.

Ethics approval and consent to participate

The ethics committee approved this study for clinical studies at Zhejiang Provincial People's Hospital. The samples were collected from volunteers and patients who provided written informed consent to a clinical study. Samples were obtained after informed consent following the ethical guidelines of the institutions.

Consent for publication

Not applicable.

Competing interests

The authors declare that they have no competing interests.

Footnotes

Publisher's Note Springer Nature remains neutral with regard to jurisdictional claims in published maps and institutional affiliations.

References

1. Floege, J., Moura, I. C. & Daha, M. R. New insights into the pathogenesis of IgA nephropathy. *Semin Immunopathol* **36**, 431-442, doi:10.1007/s00281-013-0411-7 (2014).
2. Pattrapornpisut, P., Avila-Casado, C. & Reich, H. N. IgA Nephropathy: Core Curriculum 2021. *Am J Kidney Dis* **78**, 429-441, doi:10.1053/j.ajkd.2021.01.024 (2021).
3. Suzuki, H. *et al.* Aberrantly glycosylated IgA1 in IgA nephropathy patients is recognized by IgG antibodies with restricted heterogeneity. *J Clin Invest* **119**, 1668-1677, doi:10.1172/JCI38468 (2009).
4. Barratt, J. & Tang, S. C. W. Treatment of IgA Nephropathy: Evolution Over Half a Century. *Semin Nephrol* **38**, 531-540, doi:10.1016/j.semnephrol.2018.05.023 (2018).
5. Schena, F. P. & Nistor, I. Epidemiology of IgA Nephropathy: A Global Perspective. *Semin Nephrol* **38**, 435-442, doi:10.1016/j.semnephrol.2018.05.013 (2018).
6. Wu, H. *et al.* The correlation analysis between the Oxford classification of Chinese IgA nephropathy children and renal outcome - a retrospective cohort study. *BMC Nephrol* **21**, 247, doi:10.1186/s12882-020-01913-7 (2020).

7. Barbour, S. J. *et al.* Evaluating a New International Risk-Prediction Tool in IgA Nephropathy. *JAMA Intern Med* **179**, 942-952, doi:10.1001/jamainternmed.2019.0600 (2019).
8. Cao, Y. *et al.* Decreased Expression of Urinary Mammalian Target of Rapamycin mRNA Is Related to Chronic Renal Fibrosis in IgAN. *Dis Markers* **2019**, 2424751, doi:10.1155/2019/2424751 (2019).
9. Moresco, R. N., Speeckaert, M. M. & Delanghe, J. R. Diagnosis and monitoring of IgA nephropathy: the role of biomarkers as an alternative to renal biopsy. *Autoimmun Rev* **14**, 847-853, doi:10.1016/j.autrev.2015.05.009 (2015).
10. Legouis, D. *et al.* Altered proximal tubular cell glucose metabolism during acute kidney injury is associated with mortality. *Nat Metab* **2**, 732-743, doi:10.1038/s42255-020-0238-1 (2020).
11. Zachova, K. *et al.* Galactose-Deficient IgA1 B cells in the Circulation of IgA Nephropathy Patients Carry Preferentially Lambda Light Chains and Mucosal Homing Receptors. *J Am Soc Nephrol*, doi:10.1681/ASN.2021081086 (2022).
12. Dotz, V. *et al.* - and -Glycosylation of Serum Immunoglobulin A is Associated with IgA Nephropathy and Glomerular Function. *J Am Soc Nephrol* **32**, 2455-2465, doi:10.1681/ASN.2020081208 (2021).
13. Boor, P. *et al.* Patients with IgA nephropathy exhibit high systemic PDGF-DD levels. *Nephrol Dial Transplant* **24**, 2755-2762, doi:10.1093/ndt/gfp152 (2009).
14. Floege, J., Rauen, T. & Tang, S. C. W. Current treatment of IgA nephropathy. *Semin Immunopathol* **43**, 717-728, doi:10.1007/s00281-021-00888-3 (2021).
15. Dong, R. *et al.* Studies on Novel Diagnostic and Predictive Biomarkers of Intrahepatic Cholestasis of Pregnancy Through Metabolomics and Proteomics. *Front Immunol* **12**, 733225, doi:10.3389/fimmu.2021.733225 (2021).
16. Lin, W. *et al.* Studies on diagnostic biomarkers and therapeutic mechanism of Alzheimer's disease through metabolomics and hippocampal proteomics. *Eur J Pharm Sci* **105**, 119-126, doi:10.1016/j.ejps.2017.05.003 (2017).
17. Magalhães, P., Zürbig, P., Mischak, H. & Schleicher, E. Urinary fetuin-A peptides as a new marker for impaired kidney function in patients with type 2 diabetes. *Clin Kidney J* **14**, 269-276, doi:10.1093/ckj/sfaa176 (2021).
18. Good, D. M. *et al.* Naturally occurring human urinary peptides for use in diagnosis of chronic kidney disease. *Mol Cell Proteomics* **9**, 2424-2437, doi:10.1074/mcp.M110.001917 (2010).
19. Hao, X. *et al.* Distinct metabolic profile of primary focal segmental glomerulosclerosis revealed by NMR-based metabolomics. *PLoS One* **8**, e78531, doi:10.1371/journal.pone.0078531 (2013).
20. Park, S. *et al.* Comprehensive metabolomic profiling in early IgA nephropathy patients reveals urine glycine as a prognostic biomarker. *J Cell Mol Med* **25**, 5177-5190, doi:10.1111/jcmm.16520 (2021).
21. Eddy, S., Mariani, L. H. & Kretzler, M. Integrated multi-omics approaches to improve classification of chronic kidney disease. *Nat Rev Nephrol* **16**, 657-668, doi:10.1038/s41581-020-0286-5 (2020).
22. Xia, H. *et al.* Comparative Proteomic and Metabolomic Analyses of Plasma Reveal the Novel Biomarker Panels for Thyroid Dysfunction. *Front Biosci (Landmark Ed)* **27**, 90,

doi:10.31083/j.fbl2703090 (2022).

23. Ghasemi, M. *et al.* Predictive Biomarker Panel in Proliferative Lupus Nephritis- Two-Dimensional Shotgun Proteomics. *Iran J Kidney Dis* **1**, 121-133 (2021).
24. Lai, K. N., Lai, F. M. & Vallance-Owen, J. The clinical use of serum beta-2-microglobulin and fractional beta-2-microglobulin excretion in IgA nephropathy. *Clin Nephrol* **25**, 260-265 (1986).
25. Hong, Q. *et al.* Modulation of transforming growth factor-β-induced kidney fibrosis by leucine-rich -2 glycoprotein-1. *Kidney Int* **101**, 299-314, doi:10.1016/j.kint.2021.10.023 (2022).
26. Liu, C. *et al.* Aquaporin 1 alleviates acute kidney injury via PI3K-mediated macrophage M2 polarization. *Inflamm Res* **69**, 509-521, doi:10.1007/s00011-020-01334-0 (2020).
27. Li, H. *et al.* MicroRNA-23b-3p Deletion Induces an IgA Nephropathy-like Disease Associated with Dysregulated Mucosal IgA Synthesis. *J Am Soc Nephrol* **32**, 2561-2578, doi:10.1681/ASN.2021010133 (2021).
28. Coppo, R. & Amore, A. Aberrant glycosylation in IgA nephropathy (IgAN). *Kidney Int* **65**, 1544-1547 (2004).
29. Kant, S., Kronbichler, A., Sharma, P. & Geetha, D. Advances in Understanding of Pathogenesis and Treatment of Immune-Mediated Kidney Disease: A Review. *Am J Kidney Dis* **79**, 582-600, doi:10.1053/j.ajkd.2021.07.019 (2022).
30. Xie, D. *et al.* Intensity of Macrophage Infiltration in Glomeruli Predicts Response to Immunosuppressive Therapy in Patients with IgA Nephropathy. *J Am Soc Nephrol*, doi:10.1681/ASN.2021060815 (2021).
31. Pino, L. K., Just, S. C., MacCoss, M. J. & Searle, B. C. Acquiring and Analyzing Data Independent Acquisition Proteomics Experiments without Spectrum Libraries. *Mol Cell Proteomics* **19**, 1088-1103, doi:10.1074/mcp.P119.001913 (2020).
32. Wang, Z. *et al.* Complement Activation Is Associated With Crescents in IgA Nephropathy. *Front Immunol* **12**, 676919, doi:10.3389/fimmu.2021.676919 (2021).
33. Zhong, F. *et al.* Protein S Protects against Podocyte Injury in Diabetic Nephropathy. *J Am Soc Nephrol* **29**, 1397-1410, doi:10.1681/ASN.2017030234 (2018).
34. Nelson, S. R. *et al.* Serum amyloid P component in chronic renal failure and dialysis. *Clin Chim Acta* **200**, 191-199 (1991).
35. Ning, X. *et al.* Comparative proteomic analysis of urine and laser microdissected glomeruli in IgA nephropathy. *Clin Exp Pharmacol Physiol* **44**, 576-585, doi:10.1111/1440-1681.12733 (2017).
36. Newman, A. C. *et al.* Immune-regulated IDO1-dependent tryptophan metabolism is source of one-carbon units for pancreatic cancer and stellate cells. *Mol Cell* **81**, doi:10.1016/j.molcel.2021.03.019 (2021).
37. Hsu, C.-N. & Tain, Y.-L. Developmental Programming and Reprogramming of Hypertension and Kidney Disease: Impact of Tryptophan Metabolism. *Int J Mol Sci* **21**, doi:10.3390/ijms21228705 (2020).

38. Debnath, S. *et al.* Tryptophan Metabolism in Patients With Chronic Kidney Disease Secondary to Type 2 Diabetes: Relationship to Inflammatory Markers. *Int J Tryptophan Res* **10**, 1178646917694600, doi:10.1177/1178646917694600 (2017).
39. Sallée, M. *et al.* The aryl hydrocarbon receptor-activating effect of uremic toxins from tryptophan metabolism: a new concept to understand cardiovascular complications of chronic kidney disease. *Toxins (Basel)* **6**, 934-949, doi:10.3390/toxins6030934 (2014).
40. Lattanzi, R. & Miele, R. Versatile Role of Prokineticins and Prokineticin Receptors in Neuroinflammation. *Biomedicines* **9**, doi:10.3390/biomedicines9111648 (2021).
41. Giannini, E. *et al.* The chemokine Bv8/prokineticin 2 is up-regulated in inflammatory granulocytes and modulates inflammatory pain. *Proc Natl Acad Sci U S A* **106**, 14646-14651, doi:10.1073/pnas.0903720106 (2009).
42. Maftei, D. *et al.* Controlling the activation of the Bv8/prokineticin system reduces neuroinflammation and abolishes thermal and tactile hyperalgesia in neuropathic animals. *Br J Pharmacol* **171**, 4850-4865, doi:10.1111/bph.12793 (2014).
43. Knüpfer, H. & Preiss, R. Significance of interleukin-6 (IL-6) in breast cancer (review). *Breast Cancer Res Treat* **102**, 129-135 (2007).
44. Jones, S. A. & Jenkins, B. J. Recent insights into targeting the IL-6 cytokine family in inflammatory diseases and cancer. *Nat Rev Immunol* **18**, 773-789, doi:10.1038/s41577-018-0066-7 (2018).
45. Braun, G. S. *et al.* IL-6 Trans-Signaling Drives Murine Crescentic GN. *J Am Soc Nephrol* **27**, 132-142, doi:10.1681/ASN.2014111147 (2016).
46. Huang, H., Zhang, G. & Ge, Z. lncRNA MALAT1 Promotes Renal Fibrosis in Diabetic Nephropathy by Targeting the miR-2355-3p/IL6ST Axis. *Front Pharmacol* **12**, 647650, doi:10.3389/fphar.2021.647650 (2021).
47. García-Navas, R. *et al.* Critical requirement of SOS1 RAS-GEF function for mitochondrial dynamics, metabolism, and redox homeostasis. *Oncogene* **40**, 4538-4551, doi:10.1038/s41388-021-01886-3 (2021).
48. Wei, X. *et al.* Kindlin-2 regulates renal tubular cell plasticity by activation of Ras and its downstream signaling. *Am J Physiol Renal Physiol* **306**, F271-F278, doi:10.1152/ajprenal.00499.2013 (2014).
49. Weir, N. L. *et al.* Circulating omega-7 fatty acids are differentially related to metabolic dysfunction and incident type II diabetes: The Multi-Ethnic Study of Atherosclerosis (MESA). *Diabetes Metab* **46**, 319-325, doi:10.1016/j.diabet.2019.10.005 (2020).
50. Chan, K. L. *et al.* Palmitoleate Reverses High Fat-induced Proinflammatory Macrophage Polarization via AMP-activated Protein Kinase (AMPK). *J Biol Chem* **290**, 16979-16988, doi:10.1074/jbc.M115.646992 (2015).
51. An, W. S. *et al.* Comparison of fatty acid contents of erythrocyte membrane in hemodialysis and peritoneal dialysis patients. *J Ren Nutr* **19**, 267-274, doi:10.1053/j.jrn.2009.01.027 (2009).

Figures

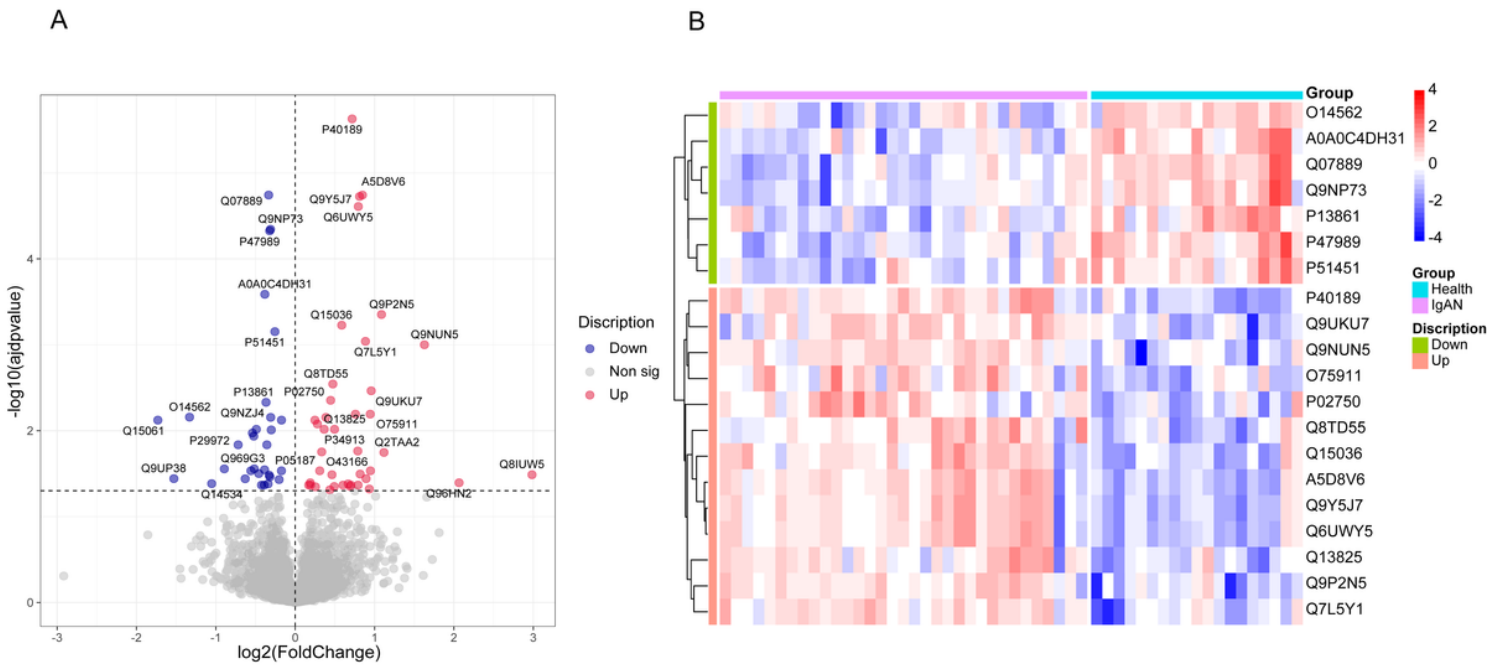

Figure 1

Proteomic analysis of IgAN. (A) The volcano plot showed DEPs between IgAN and health control. The red points represented 40 proteins that were up-regulated in the IgAN group (adjusted P < 0.05). The blue points represented 31 proteins that were down-regulated in the IgAN group (adjusted P value < 0.05) (B) The levels of DEPs in samples were analyzed by hierarchical clustering analysis. The heat map represented the Z scores of the top 20 DEPs in the IgAN group. (Red represents up-regulated, and blue represents down-regulated).

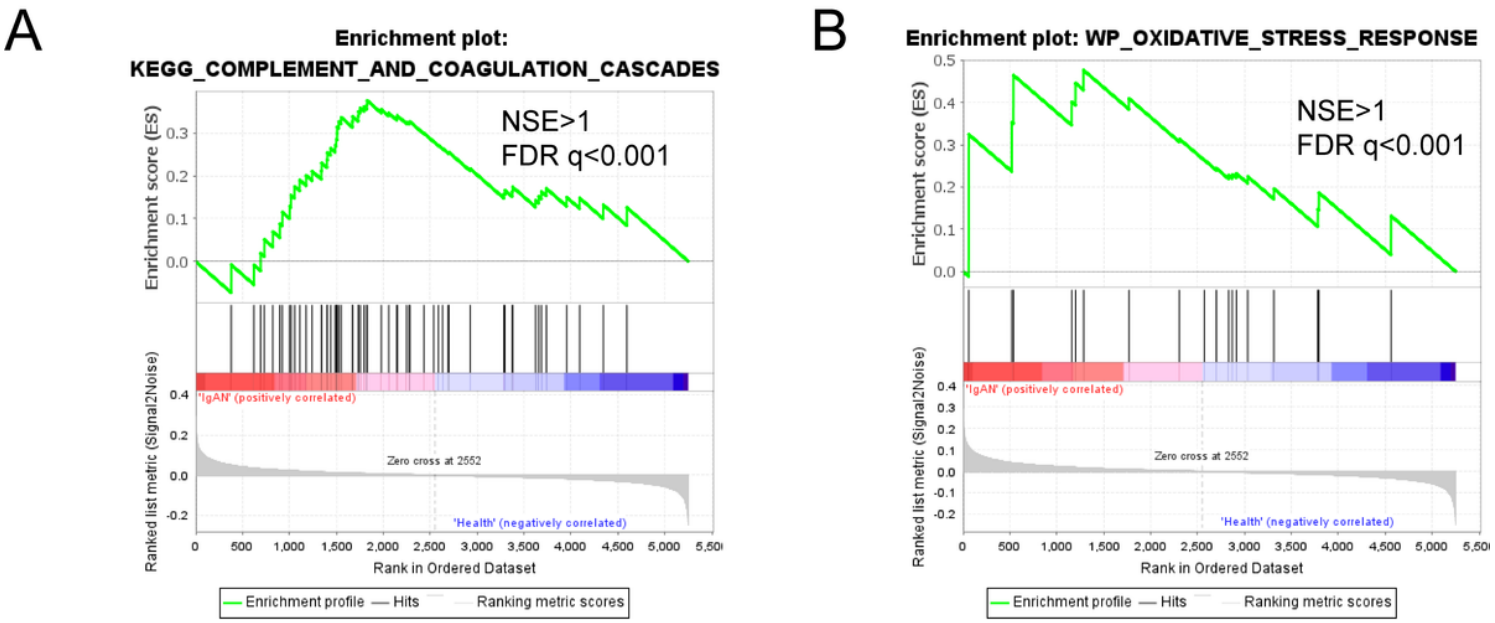

Figure 2

GSEA gene sets Enriched gene sets detected by GSEA in IgAN. (A-B) GSEA plots indicated significant enrichment of complement and coagulation cascades, and oxidative stress response in the IgAN compared with the healthy group. Genes were ordered according to their ranked ratios, and GSEA was performed using the GSEA (version 4.2.3) tool. The plot (green curve) shows the enrichment score (ES), for ranked genes compared with complement and coagulation cascades, and oxidative stress response gene set. The normalized enrichment scores (NESs) and false discovery rate (FDR) q-values (FDR q) were indicated.

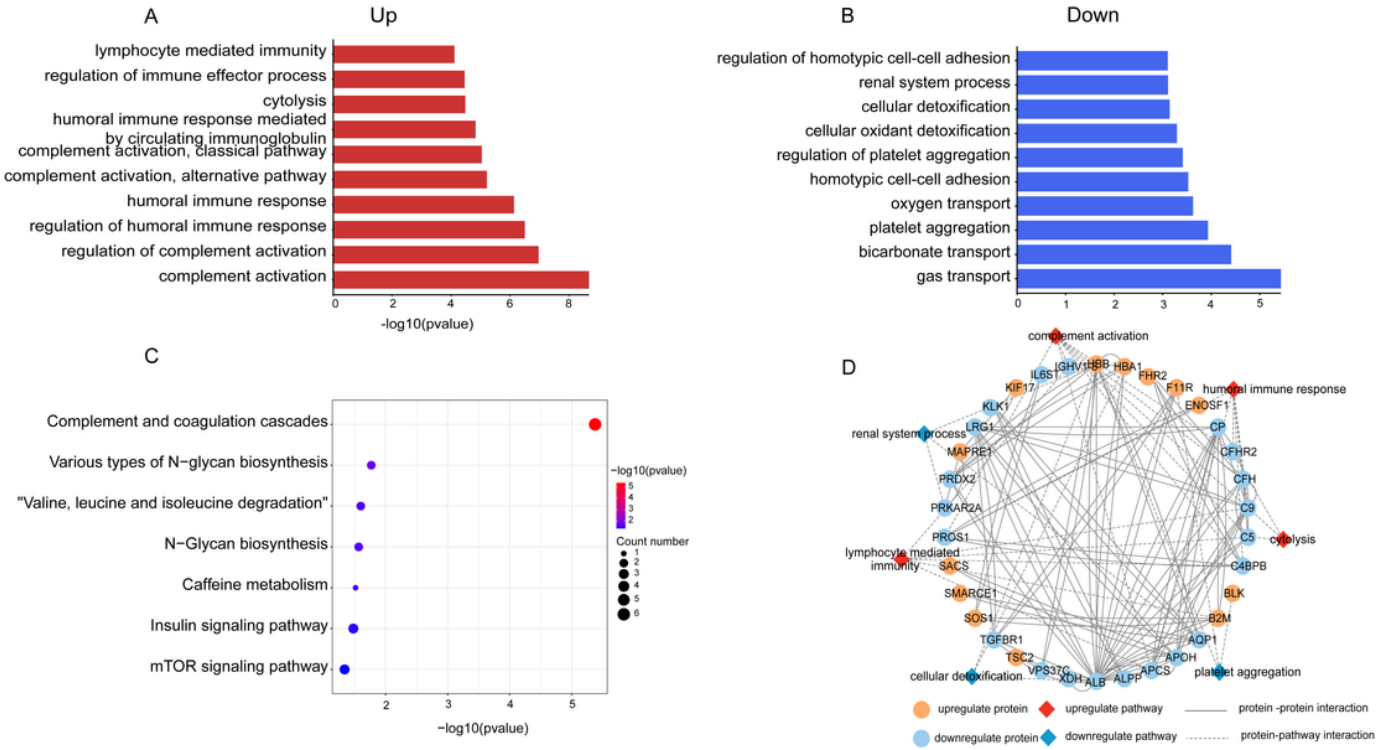

Figure 3

GO terms and KEGG pathway analysis for DEPs. (A) Up-regulated biological processes. GO annotation-biological processes enriched by up-regulated DEPs in IgAN. (B) Down-regulated biological processes. GO annotation-biological processes enriched by down-regulated DEPs in IgAN. (C) Enriched KEGG pathways of DEPs. (D) Proteins-pathways-proteins interaction network. Significantly altered biological process pathways were involved in the protein-protein interaction network of DEPs. GO, Gene Ontology; KEGG, Kyoto Encyclopedia of Genes and Genomes.

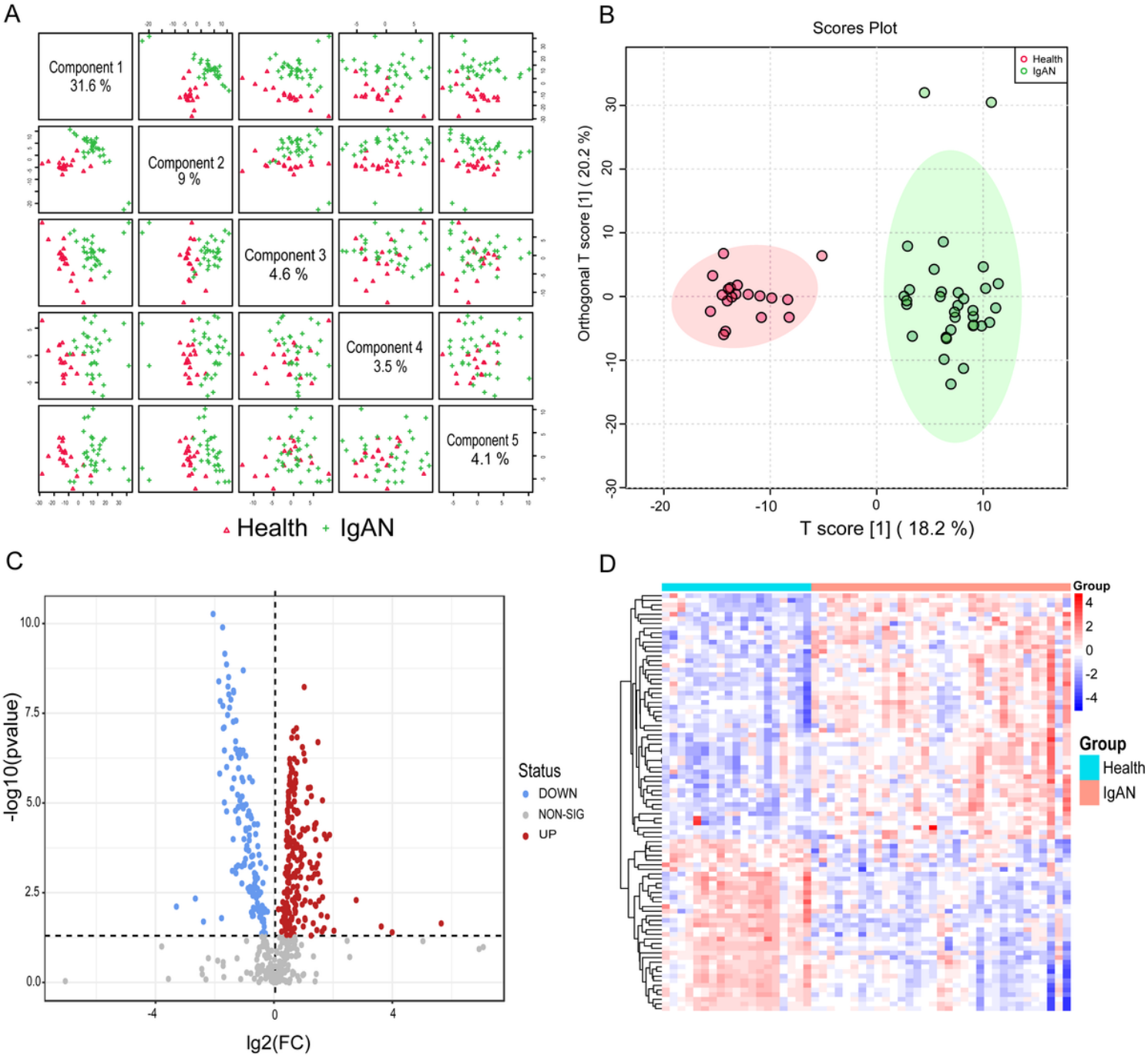

Figure 4

Multivariate data analysis of IgAN metabolomics data. (A) Principal Component (PC) scores plot from PLS-DA model. The diagonal shown the pairwise scoring plots between the five principal components with the corresponding variances. (B) OPLS-DA score plot showed the separation between the control group and IgAN. (C) Volcano plot of DEMs. The red points represented up-regulated metabolites, and the blue points represented down-regulated metabolites in the IgAN group. (D) Heat map presenting DEMs between the IgAN and control groups. (Red represents up-regulated, and blue represents down-regulated in the IgAN group).

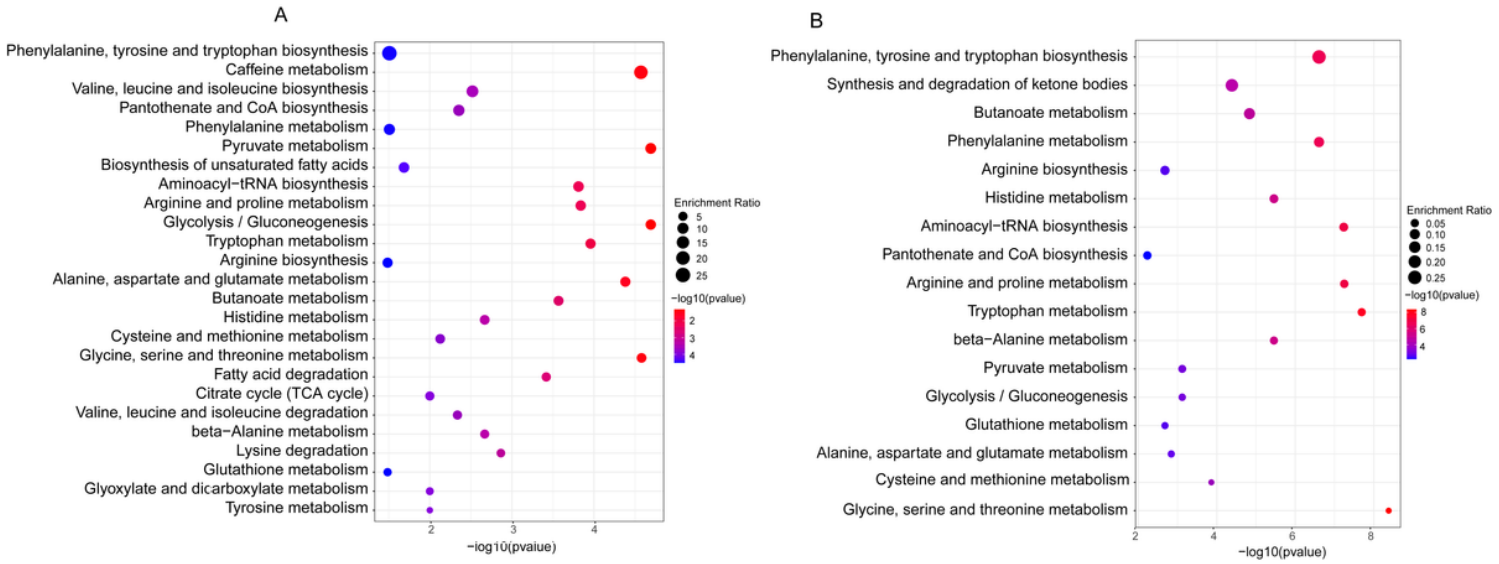

Figure 5

Enrichment analysis of metabolites using Metabolanalyst 5.0 online software. (A) The metabolome set enrichment analysis (MSEA) for identifying significantly altered metabolic pathways. (B) KEGG pathway enrichment analysis of DAMs. ($P < 0.05$; VIP-Scores >1)

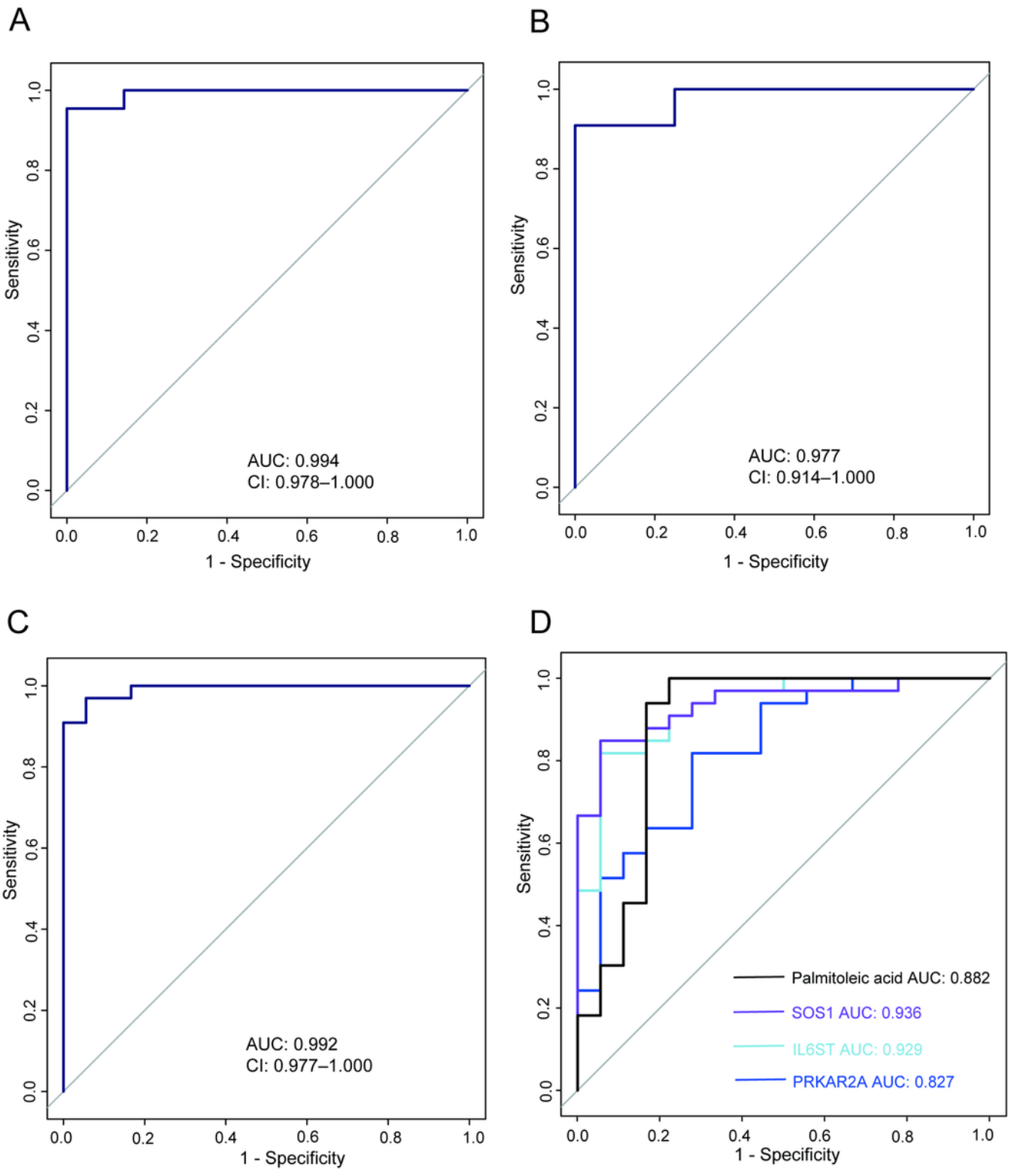

Figure 6

The diagnostic efficacy of biomarkers in IgAN. (A) ROC analysis of the combined model was performed to evaluate the diagnostic performance in the training set. (B) ROC analysis of the combined model was performed to assess the diagnostic performance in the testing set. (C) ROC analysis of the combined model was performed to evaluate the diagnostic performance in the entire collection. (D) ROC analysis of

the four biomarkers was performed to evaluate the diagnostic performance in the entire collection, respectively.

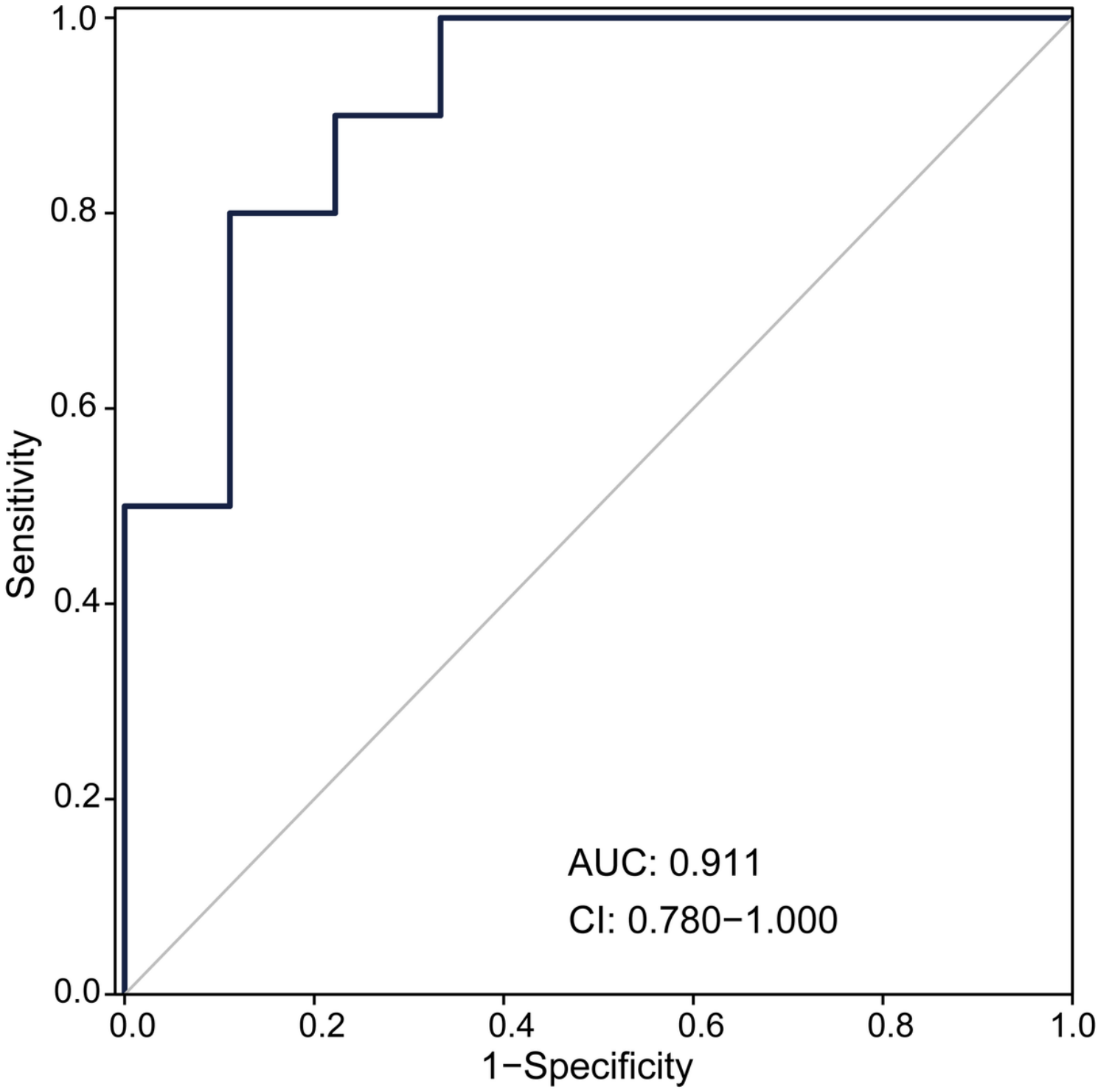

Figure 7

ROC analysis in the validation set. The performance of the combined diagnostic model in the validation set was evaluated by ROC analysis.

Supplementary Files

This is a list of supplementary files associated with this preprint. Click to download.

- Supplementfigure.doc
- Supplementtable.doc